

## CIVA-Stabilized Finite Element Method for Tsunami Simulations

\*Yusuke Takahashi<sup>1</sup>, Masaaki Sakuraba<sup>2</sup>, and Kazuo Kashiwama<sup>1</sup>

<sup>1</sup> Department of Civil and Environmental Engineering, Chuo University, Kasuga 1-13-27, Bunkyo-ku, Tokyo, Japan

<sup>2</sup> Disaster Prevention Hydraulics Group, Nippon Koei Co., Ltd., 2304 Inarihara, Tsukuba-shi, Ibaraki 300-1259, Japan

\*Corresponding author: takahashi@civil.chuo-u.ac.jp

### Abstract

This paper presents a numerical method using the CIVA-stabilized finite element method based on SUPG (CIVA-SUPG) for tsunami simulations. The Boussinesq equation is employed for the governing equation in order to treat both the wave nonlinearity and dispersion effects. The equation is divided into two phases, an advection phase and a non-advection phase. The CIVA method is employed to the advection phase and the stabilized finite element method based on SUPG is employed to the discretization for non-advection phase. The present method is applied to several benchmark examples to show the validity and efficiency of the method. For the application example, the present method is employed to the tsunami simulation generated by Great East-Japan earthquake.

**Keywords:** CIVA-SUPG finite element method, Tsunami, Boussinesq equation, Wave run-up

### Introduction

A number of flood disasters by tsunami occur in various parts of the world. The flood disasters by tsunami waves cause the enormous damage to the human life and economic activities. In order to estimate the extent of the disaster quantitatively, it is important to use accurate numerical method for tsunami waves. The two-dimensional shallow water equation and the Boussinesq equation are normally used for the governing equation for tsunami waves. The shallow water equation can describe the wave nonlinearity, however, the wave dispersion effect is not considered in the shallow water equation. On the other hand, Boussinesq equation can treat both the wave nonlinearity and dispersion effects, the equation is suitable for the governing equation for tsunami simulation.

For the tsunami numerical simulation, a number of numerical methods have been proposed. The finite difference is well used. However, it is necessary to use the nesting techniques in order to use the fine grid at the nearshore area since the regular grid is employed in the finite difference method. On the other hand, the finite element method does not need the nesting techniques since the unstructured grid is employed. Therefore, the finite element method is suitable for tsunami simulation since that can treat the complicated geometry easily.

This paper presents a numerical method using the CIVA-stabilized finite element method based on SUPG (CIVA-SUPG) for tsunami simulations. The Boussinesq equation is employed for the governing equation. The governing equation is divided into two phases, an advection phase and a non-advection phase. The CIVA method (Tanaka, 1999) is employed to the advection phase and the stabilized finite element method based on SUPG (Takase et al, 2010) is employed to the discretization for non-advection phase. The moving boundary technique based on fixed grid is employed. The present method is applied to several numerical examples to show the validity and efficiency of the method. For the application example, the present method is applied to the tsunami simulation generated by Great East-Japan earthquake using an unstructured triangular grid with the element Courant number constant.

### Governing Equations

For the governing equation, the Boussinesq equation is employed. This equation can treat the wave nonlinearity and dispersion effects. The governing equation can be described as follows:

$$\frac{\partial H}{\partial t} + \frac{\partial(u_i H)}{\partial x_i} = 0 \quad (1)$$

$$\frac{\partial(u_i H)}{\partial t} + \frac{\partial(u_j u_i H)}{\partial x_j} + gH \frac{\partial(H+z)}{\partial x_i} + \frac{gn^2 u_i \sqrt{u_j u_j}}{\partial x_i} + \frac{\partial}{\partial x_i} \left( \frac{h^2}{3} \frac{\partial(u_j H)}{\partial t \partial x_j} \right) = 0 \quad (2)$$

Where  $H$ ,  $u_i$ ,  $g$ ,  $z$  and  $n$  are total water depth, depth averaged velocity, acceleration of gravity, still water depth, bed slope and Manning's coefficient, respectively.

The governing equation can be divided into two phases as below:

$$\frac{\partial(u_i H)}{\partial t} + u_j \frac{\partial(u_i H)}{\partial x_j} = 0 \quad (3)$$

$$\frac{\partial H}{\partial t} + \frac{\partial(u_i H)}{\partial x_i} = 0 \quad (4)$$

$$\frac{\partial(u_i H)}{\partial t} + (u_i H) \frac{\partial u_j}{\partial x_j} + gH \frac{\partial(H+z)}{\partial x_i} + \frac{gn^2 u_i \sqrt{u_j u_j}}{\partial x_i} + \frac{\partial}{\partial x_i} \left( \frac{h^2}{3} \frac{\partial(u_j H)}{\partial t \partial x_j} \right) = 0 \quad (5)$$

Eq. (3) is equation of advection phase (advection equation), the Eq. (4) and (5) are equations of non-advection phase.

## Numerical methods

### Advection Phase

The solution of Eq. (3) for advection phase is computed by the CIVA method (Cubic Interpolation with Volume/Area co-ordinates) proposed by Tanaka (1999). The method is an extended method of CIP for unstructured-grid, and the solution for advection equation is solved by the cubic interpolation as:

$$f(L_1, L_2, L_3) = \sum_{i=1}^3 \alpha_i L_i + d \sum_{i=1}^3 \beta_{jk} \left( L_j^2 L_k + \frac{1}{2} L_1 L_2 L_3 \right) \quad (6)$$

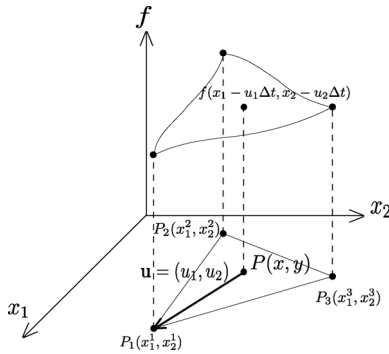


Figure 1. CIVA method

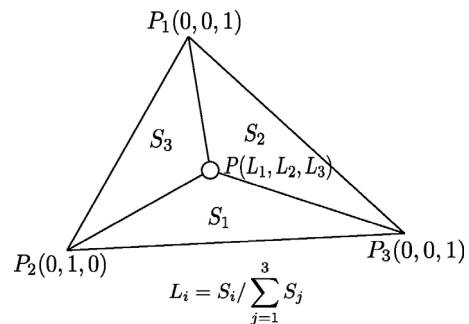


Figure 2. Area coordinate

Where,  $f$  is the discharge fluxes  $u_i H$  for  $x_i$  directions and  $L_i$  is the area coordinates (see Fig. 2). In order to compute the nodal value at P1 at time level n+1, the position of node P1 at time level n

(Point P) is determined by using the velocity at time level n. Then, the value at point P is obtained by Eq. (3) using three nodal values at time level n. The computed value is transported to point P at time level n+1. (see Fig.1)

### Non-advection Phase

After the advection phase, Eqs. (4), (5) are discretized by the stabilized finite element method based on SUPG method (Streamline-Upwind Petrov Galerkin) using the results of the advection phase. Eqs. (4), (5) can be expressed by the vector form as follows:

$$\frac{\partial \mathbf{U}}{\partial t} + \mathbf{A}_i \frac{\partial \mathbf{U}}{\partial x_i} - \mathbf{R} + \mathbf{G}\mathbf{U} + \frac{\partial^2}{\partial t \partial x_i} (\mathbf{K}) = 0 \quad (7)$$

$$\mathbf{U} = \begin{bmatrix} H \\ u_1 H \\ u_2 H \end{bmatrix}, \quad \mathbf{R} = \begin{bmatrix} 0 \\ -c^2 \frac{\partial z}{\partial x_1} \\ -c^2 \frac{\partial z}{\partial x_2} \end{bmatrix}, \quad \mathbf{K} = \begin{bmatrix} 0 \\ -\frac{h^2}{3} \left( \frac{\partial(\overline{u_1 H})}{\partial x_1} + \frac{\partial(\overline{u_2 H})}{\partial x_2} \right) \\ -\frac{h^2}{3} \left( \frac{\partial(\overline{u_1 H})}{\partial x_1} + \frac{\partial(\overline{u_2 H})}{\partial x_2} \right) \end{bmatrix},$$

$$\mathbf{A}_1 = \begin{bmatrix} 0 & 1 & 0 \\ c^2 - \overline{u_1^2} & \overline{u_1} & 0 \\ -\overline{u_1 u_2} & \overline{u_2} & 0 \end{bmatrix}, \quad \mathbf{A}_2 = \begin{bmatrix} 0 & 0 & 1 \\ -\overline{u_1 u_2} & 0 & \overline{u_1} \\ c^2 - \overline{u_2^2} & 0 & \overline{u_2} \end{bmatrix}, \quad \mathbf{G} = \begin{bmatrix} 0 & 0 & 0 \\ 0 & \frac{u_*}{H} & 0 \\ 0 & 0 & \frac{u_*}{H} \end{bmatrix}, \quad u_* = \frac{gn^2}{H^{1/3}} \sqrt{\overline{u_1^2} + \overline{u_2^2}}$$

Here  $\mathbf{U}$ ,  $\mathbf{R}$ ,  $\mathbf{K}$ ,  $\mathbf{A}_i$  and  $\mathbf{G}$  are unknown vector, bed slope term, dispersion term, nonlinear term and friction term respectively. The valuables with overline are the computed results by the advection phase. Applying the stabilized finite element method to Eq. (7), the weighted residuals equation is given as follows:

$$\int_{\Omega} \mathbf{U}^* \cdot \left( \frac{\partial \mathbf{U}}{\partial t} + \mathbf{A}_i \frac{\partial \mathbf{U}}{\partial x_i} - \mathbf{R} + \mathbf{G}\mathbf{U} \right) d\Omega + \int_{\Omega} \left( \frac{\partial \mathbf{U}^*}{\partial x_i} \right) \cdot \left( \frac{\partial}{\partial t} (\mathbf{K}) \right) d\Omega$$

$$+ \sum_{e=1}^{n_{el}} \int_{\Omega} \tau(\mathbf{A}_i) \left( \frac{\partial \mathbf{U}^*}{\partial x_i} \right) \cdot \left( \frac{\partial \mathbf{U}}{\partial t} + \mathbf{A}_i \frac{\partial \mathbf{U}}{\partial x_i} - \mathbf{R} + \mathbf{G}\mathbf{U} \right) d\Omega \quad (8)$$

$$+ \sum_{e=1}^{n_{el}} \int_{\Omega} \delta \left( \frac{\partial \mathbf{U}^*}{\partial x_i} \right) \cdot \left( \frac{\partial \mathbf{U}}{\partial x_i} \right) d\Omega = \int_{\Gamma} \mathbf{U}^* \cdot \mathbf{T} d\Gamma$$

Here  $\tau$  is the SUPG stabilization parameter,  $\delta$  is the shock-capturing parameter. In Eq. (8), the first term, second term and right hand side term are Galerkin terms, the third term are SUPG stabilization terms, the fourth terms are shock-capturing term. For the spatial discretization, the continuous linear interpolation element is employed. For the discretization in time, the implicit method based on Crank-Nicolson method is employed.

### *Moving Boundary Techniques*

In order to describe the behavior of the tsunami run-up and run-off, the Eulerian approach using fixed grid is employed for the moving boundary condition. Fig. 3 shows the definition sketch for the treatment of moving boundary. Every nodal water depth is compared with the small water depth  $\epsilon$  at every time step. Each element is classified into three types; wet, dry or partial wet element (Kawahara and Umetsu (1986)).

- Wet element : The water depth for all three nodes are greater than  $\epsilon$ . The element is included in the computational area.
- Dry element : The water depth for all three nodes are smaller than  $\epsilon$ . The element is omitted from the computational area. The nodal velocity is assumed to be zero.
- Partial wet element : The water depth for one or two nodes are greater than  $\epsilon$ . The element is included in the computational area. The nodal velocity is assumed to be zero and the water depth is assumed to be  $\epsilon$  for the node located on dry bed.

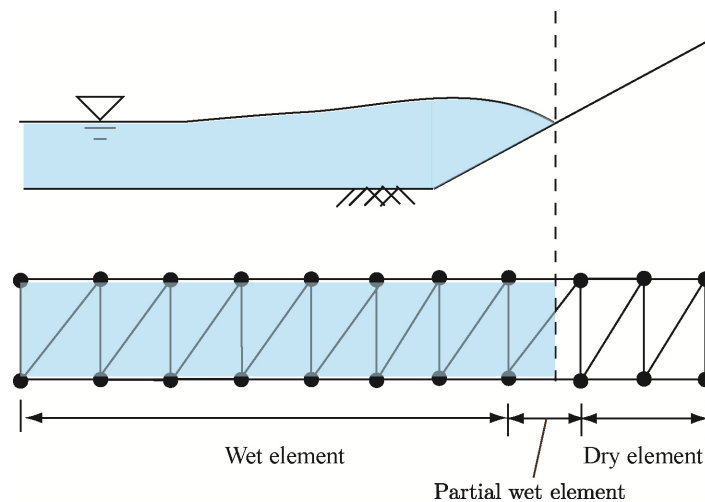


**Figure 3. Moving boundary technique**

### **Numerical Examples**

The present method is applied to several numerical examples to investigate the validity and efficiency.

#### *Dam-break Problem*

The present method is applied to dam-break problem in the rectangular tank. The computational model and initial water depth are shown in Fig. 4. The dam is broken instantaneously at time  $t = 0s$ . In this problem, the shallow water equation is employed for the governing equation in order to investigate the numerical accuracy comparing with the theoretical result. For the numerical condition, the time increment is assumed to be 0.001sec. For the boundary condition, the slip boundary condition is set to the wall.

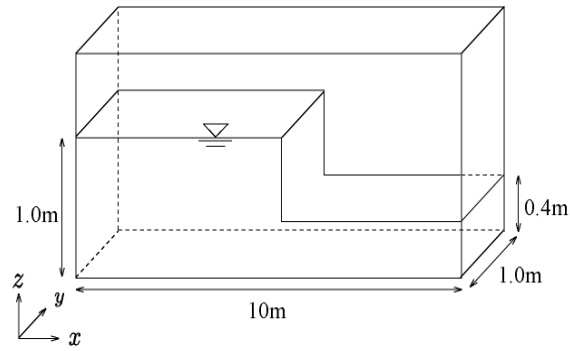


**Figure 4. Computational model**

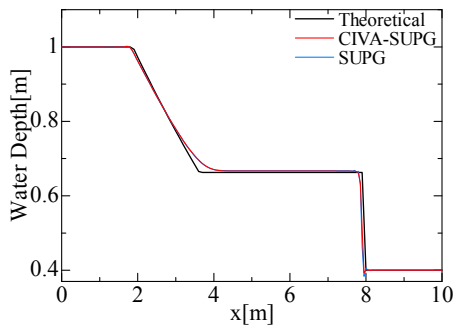


**Figure 5. Computed water depth**

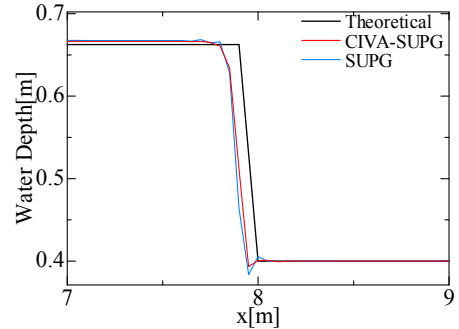
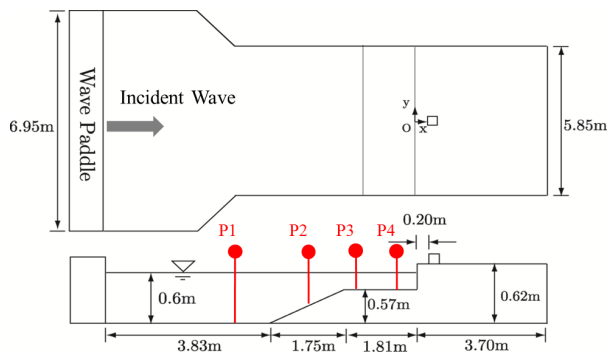


**Figure 6. Zoom up around  $x=8.0m$**

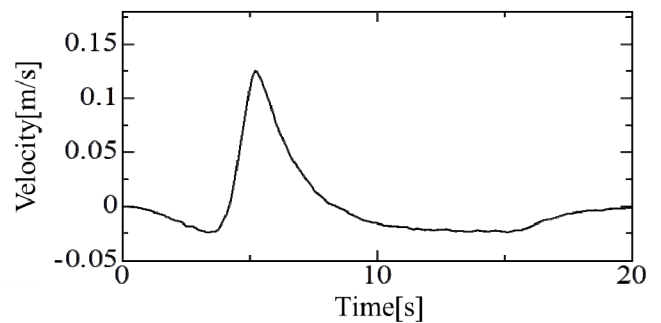
Fig. 5 shows the comparison with the theoretical solution for water depth at time  $t = 1s$ . Fig. 6 shows the zoom-up around  $x = 8.0m$ . The computed results obtained by the present method are in good agreement with the results obtained by the SUPG method (Takase et al, 2010).

### *Tsunami Run-up Problem*

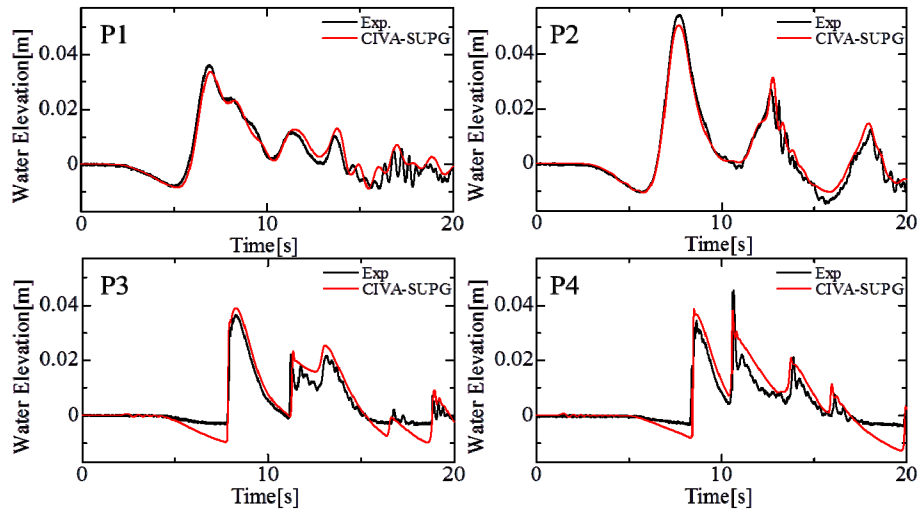
The present method is applied to a tsunami run-up problem in the tank. Fig.7 shows the computational model which is used by the experiment by National Defence Academy of Japan (Fujima et al, 2009). The wave paddle moves to make the incident wave. Fig. 8 shows the time history of velocity of paddle which is applied to the boundary condition for the velocity for  $x_1$  direction at the paddle. The slip boundary condition is set to other walls. For the numerical condition, the time increment is assumed to be 0.005s and the Manning's coefficient is assumed  $0.01 m/s^{1/3}$ . The computed results were compared with the experimental data at the observation points of P1, P2, P3 and P4 (see Fig. 7).



**Figure 7. Computational model**



**Figure 8. Velocity of wave paddle**



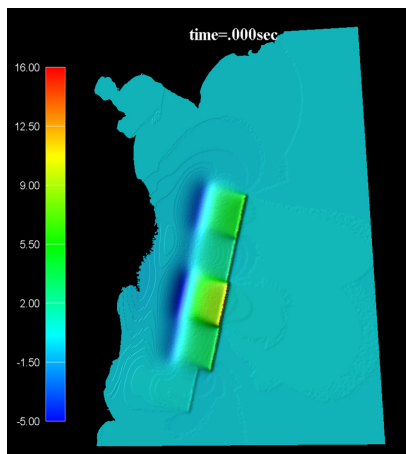
**Figure 9. Comparison with the experimental results at the observation points**

Fig. 9 shows the comparison of water elevation with the experimental results at the observation points P1-P4. From this figure, the computed results by the present method are in good agreement with the experimental results at all observation points.

#### *Tsunami Simulation by the Great East Japan Earthquake*

The present method is applied to tsunami run-up simulation by the Great East-Japan Earthquake as the application example. The unstructured triangular mesh with the element Courant number constant is employed. The initial water surface displacement is given by the faults model proposed by Mansinha and Smylie (1971). The fault data proposed by Tohoku University Ver. 1.0 ([http://www.tsunami.civil.tohoku.ac.jp/hokusai3/J/events/tohoku\\_2011/model/](http://www.tsunami.civil.tohoku.ac.jp/hokusai3/J/events/tohoku_2011/model/)), is employed. Fig. 10 shows the computational domain and the initial condition for water elevation. Time increment is assumed to be 0.1s. The non-slip boundary condition is employed at the coastline and the open boundary condition is employed at the open boundary. The treatment method for moving boundary is employed at the land area. In this simulation, we focus on the Onagawa area because the area had big damage by tsunami.

Fig. 11 shows the computed results at time = 900s. The wave dispersive effect is clearly shown in the results.



**Figure 10. Initial condition**

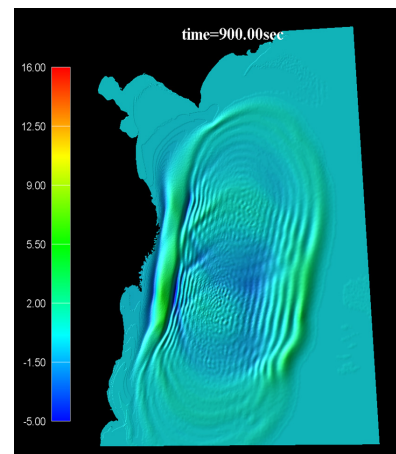


**Figure 11. Wave propagation (time=900sec)**

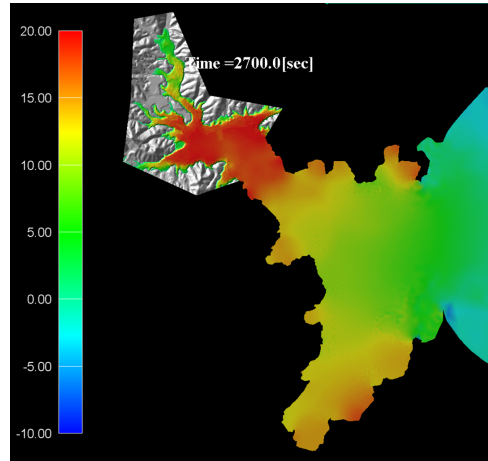
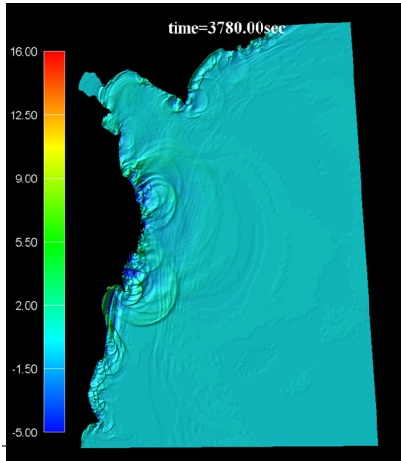


**Figure 12. Wave propagation and run-up at Onagawa (time=2700s)**

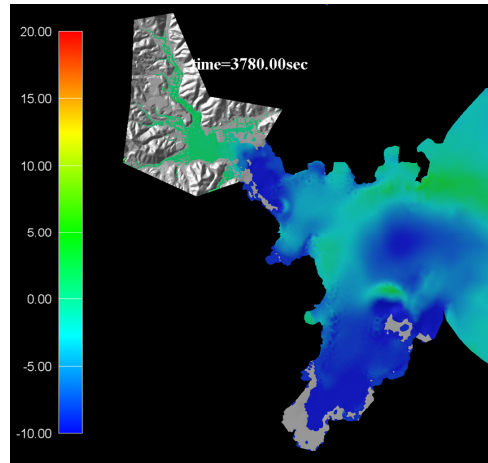
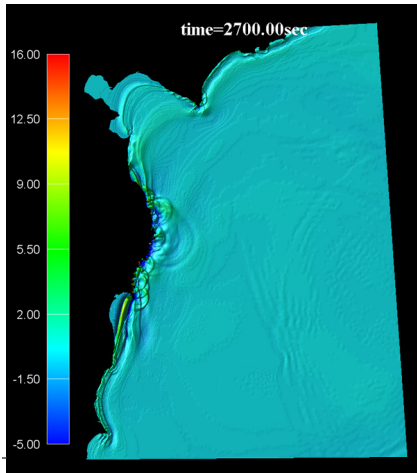


**Figure 13. Wave propagation and run-off at Onagawa (time=3780s)**

Fig. 12 shows the computed wave propagation (left) and the run-up at Onagawa area (right) at time =2700s, which is the state that the maximum water elevation is observed at Onagawa by first tsunami wave. Fig. 13 shows the computed wave propagation (left) and the run-off at Onagawa area (right) at time =3780s, which is the state that the minimum water elevation is observed at Onagawa by first tsunami.

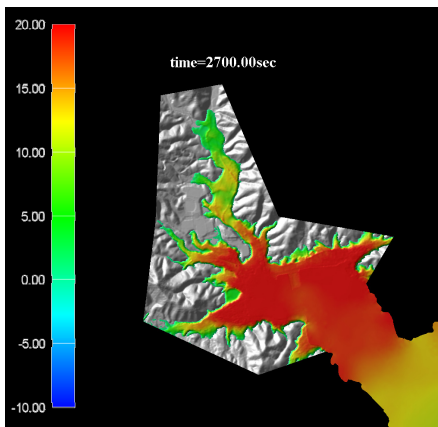


**Figure 14. Computed inundation area**

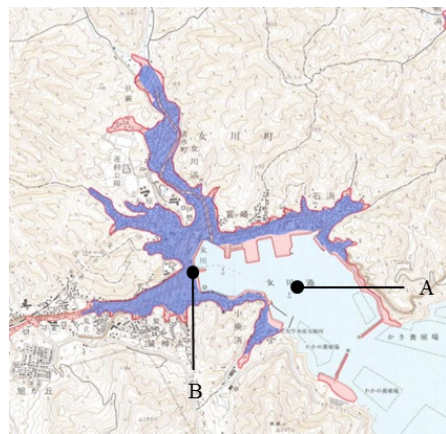


**Figure 15. Tsunami damaged area**

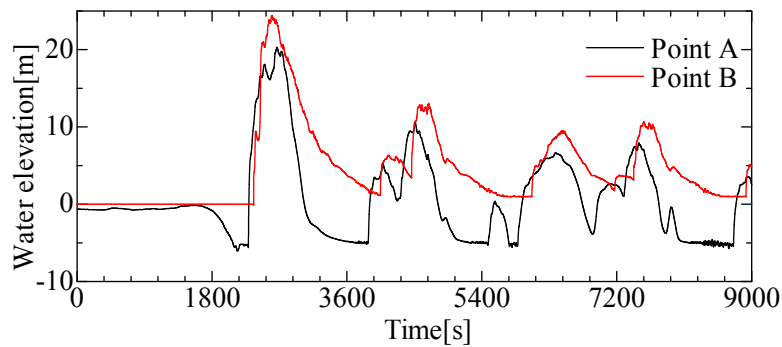


**Figure 16. Time history of water elevation at point A and B**

Fig.14 shows the computed inundation area by the first wave in Onagawa. Fig. 15 shows the investigation map of tsunami damaged area at Onagawa. The red area shows the inundation area and the blue area shows the building damaged area. The computational result is good agreement with the observed data. Fig.16 shows the time history of water elevation at the observation points A and B in Fig. 15. From the figure, the maximum water elevation over 20m is obtained at time = 2700s.

## Conclusions

The CIVA-stabilized finite element method has been presented for tsunami simulation. The Boussinesq equation is employed for governing equation. In order to show the validity and efficiency, the present method is applied to several numerical examples. From the results, the following conclusions are obtained.

For the dam break problem, the computed results by CIVA-SUPG finite element method are good agreement with the theoretical results comparing with the stabilized finite element method based on SUPG. For the tsunami run-up problem, the computed results by present method are good agreement with the experimental results.

For the application example by the Great East Japan Earthquake, the computed inundation area is good agreement with the observed data.

From the results in this paper, it can be concluded that the present method is useful for tsunami simulation.

We plan to consider the effect of collapse of building in future works.

## References

- Tanaka, N. (1999), Development of a highly accurate interpolation method for mesh-free flow simulations I. Integration of gridless, particle and CIP methods, *International Journal for Numerical methods in Fluids*, 30, pp. 957-976.
- Takase, S., Kashiyama, K. , Tanaka and S. Tezduyar, T. E. (2010), Space-time SUPG formulation of the shallow-water equations, *International Journal for Numerical methods in Fluids*, 64, pp. 1379-1394.
- Fujima, K., Achmad, F., Shigihara, Y. and Mizutani, N. (2009), Estimation of tsunami force acting on rectangular structures, *Journal of Disaster Research*, 4, pp. 404-409.
- Mansinha, L. and Smylie D. E. (1971), The displacement fields of inclined faults, *Bullet of the Seismological Society of America*, 61, pp.1433-1440.
- Kawahara, M. and Umetsu, T. (1986), Finite element method for moving boundary problems in river flow, *International Journal of Numerical Methods in Fluids*, pp.163-186.